

## Case Report

# FDG PET imaging in multiple myeloma: implications for response assessments in clinical trials

Suchitra Sundaram<sup>1</sup>, James Driscoll<sup>2,3</sup>, Mariano Fernandez-Ulloa<sup>4</sup>, Marcos de Lima<sup>1</sup>, Ehsan Malek<sup>1</sup>

<sup>1</sup>University Hospitals, Case Comprehensive Cancer Center, Case Western Reserve University, Cleveland, OH, USA;

<sup>2</sup>Division of Hematology and Oncology, <sup>3</sup>The Vontz Center for Molecular Studies, <sup>4</sup>Division of Nuclear Medicine, University of Cincinnati College of Medicine, Cincinnati, OH, USA

Received May 31, 2018; Accepted November 15, 2018; Epub December 20, 2018; Published December 30, 2018

**Abstract:** <sup>18</sup>F-fluorodeoxyglucose positron emission tomography integrated with computed tomography (<sup>18</sup>F-FDG PET/CT) is an effective modality to assess disease burden, detect extra-medullary disease and monitor minimal residual disease (MRD) for multiple myeloma (MM) patients. This modality of imaging is incorporated in the International Myeloma Working Group (IMWG) response criteria that are widely used in MM clinical trials. Interpretative pitfalls are commonly encountered in <sup>18</sup>F-FDG PET/CT studies and proper interpretation requires knowledge of the normal physiologic distribution of the tracer affecting available <sup>18</sup>F-FDG for tumor tissue uptake. We describe a series of MM patients who exhibited a deep response to treatment, based on clinical features, serum markers and bone marrow (BM) biopsy. However, these patients seemed to have new lesions on post-therapy <sup>18</sup>F-FDG PET/CT images which could be interpreted as progressive disease according to the IMWG criteria. Sequestration phenomenon, which is the disappearance of <sup>18</sup>F-FDG sequestration by myeloma-infiltrated marrow after successful anti-myeloma therapy, could lead to unmasking of new <sup>18</sup>F-FDG-avid lesions on post-therapy PET/CT due to higher <sup>18</sup>F-FDG bioavailability to residual tumor tissue. Clinical correlation, awareness of the <sup>18</sup>F-FDG sequestration in myeloma infiltrated BM and its impact on other <sup>18</sup>F-FDG avid areas in the body are necessary to avoid potential pitfalls in end-of-treatment imaging interpretation. While considering patients for clinical trials, clinicians should be mindful of this sequestration phenomenon in the interpretation of post-therapy PET/CT imaging in MM patients with initially heavily infiltrated marrow.

**Keywords:** FDG PET imaging, multiple myeloma, clinical trials

## Introduction

<sup>18</sup>F-FDG PET/CT is commonly used for the detection of myeloma bone disease and extra-medullary sites of metabolically active myeloma foci with relatively high sensitivity and specificity. Furthermore, follow-up PET/CT scans can be used to monitor treatment response and are of prognostic value for survival [1-3]. This modality of imaging uses enhanced glucose metabolic activity to visualize areas of interest, and detects more lesions compared to whole body X ray [4, 5]. A decrease in <sup>18</sup>F-FDG uptake correlates with chemotherapeutic response, and residual <sup>18</sup>F-FDG uptake after completion of therapy may serve as an accurate marker for assessing MRD comparable to next-generation sequencing or multi-color flow cytometry [6, 7]. According to the IMWG response criteria, development of new bony lesions or soft tissue plas-

macytoma on imaging modalities, including PET/CT indicates progressive disease (PD) independent of serum monoclonal protein or light chain concentration [8, 9]. This criterion is widely used in myeloma clinical trials to unify the trial recruitment and response assessment across studies. However, cautious interpretation of the PET/CT findings is necessary, taking into consideration the possible pitfalls encountered due to normal variation, processes that mimic pathology and factors influencing the <sup>18</sup>F-FDG distribution throughout the body [10, 11]. Here, we present a series of cases highlighting the phenomenon of <sup>18</sup>F-FDG sequestration by heavily myeloma-infiltrated BM at diagnosis, which can lead to false interpretation of residual disease as PD on subsequent PET/CT images when patients experienced a significant response.

# PET imaging in multiple myeloma

**Table 1.** Patient demographics and clinical characteristics

Clinical Parameters	Case 1	Case 2	Case 3
Age (years)	61	69	65
Gender	Male	Male	Male
Type of para protein	IgG Lambda	IgG Kappa	IgA Lambda
Stage (r-ISS)	III	III	II
CRAB criteria	Anemia Lytic lesions	Anemia Renal failure	Anemia Hypercalcemia
Pre-therapy BM cellularity (%)	65	45	30
Pre-therapy myeloma involvement of BM (%)	90	60	95
Cytogenetics	Hyperdiploidy	t (11; 14)	Hyperdiploidy
Risk stratification	Standard risk	Standard risk	Standard risk
Pre-therapy FDG PET	1. Widespread BM uptake 2. Uptake in extremities	1. Widespread BM uptake 2. Low brain uptake	1. Widespread BM uptake 2. Liver lesion
Pre-therapy serum M-spike	3.2 gm/dL	5.4 gm/dL	4.6 gm/dL
Type of Chemotherapy	Carfilzomib Pomalidomide Dexamethasone Daratumumab Elotuzumab	Bortezomib Lenalidomide Dexamethasone	Bortezomib Lenalidomide Dexamethasone Cisplatin Doxorubicin Cyclophosphamide Etoposide Thalidomide Daratumumab Carfilzomib
Post-therapy serum M-spike	0.2 gm/dL	0.1 gm/dL	0.2 gm/dL
Post-therapy PET uptake in BM	No uptake	No uptake	No uptake
Post-therapy PET	1. Right humerus 2. Left femur	1. Right femur 2. Increased brain uptake	1. Appendicular skeleton 2. Pelvic lesions
Post-therapy BM cellularity (%)	35	30	50
Post-therapy BM MM burden (%)	0	10	10-20

MM - multiple myeloma, r-ISS - Revised International Staging System, CRAB - hypercalcemia, renal failure, anemia and bone lesions (CRAB criteria signify the presence of end-organ damage in multiple myeloma), BM - bone marrow, M-spike - measurable marker of multiple myeloma in blood.

## Materials and methods

### <sup>18</sup>F-FDG acquisition and evaluation

Our series consisted of three patients diagnosed with MM according to the IMWG criteria and underwent staging according to the Revised International Staging System [12]. All patients underwent whole body <sup>18</sup>F-FDG PET/CT for initial diagnosis of the disease according to standard protocol in our center. After a fasting period of at least 4 hours, patients received an intravenous dose of 13.7 mCi of <sup>18</sup>F-FDG. PET images from skull vertex to feet were then acquired after a one hour delay. Also acquired was a contemporaneous low dose non-contrast CT scan performed for attenuation correction of PET images and anatomic localization. The PET and CT images were digitally fused for display and all images were acquired on a combined PET-CT scanner unit. Bone and extramedullary lesions with a Deauville score  $\geq 4$  on PET scan were identified

as positive foci of disease involvement and selected as index lesions for assessment post-therapy.

### Informed consent

Informed consent for the study was obtained from each patient described in our series. In accordance with our institutional policy for a short case series, institutional review board (IRB) review and approval was not deemed necessary for publication.

### Presentation and management of cases

In **Table 1**, we summarize the clinical features of each patient with their disease characteristics and treatment received.

#### Case 1

61-year-old male diagnosed with ISS Stage III MM underwent standard triplet induction ther-

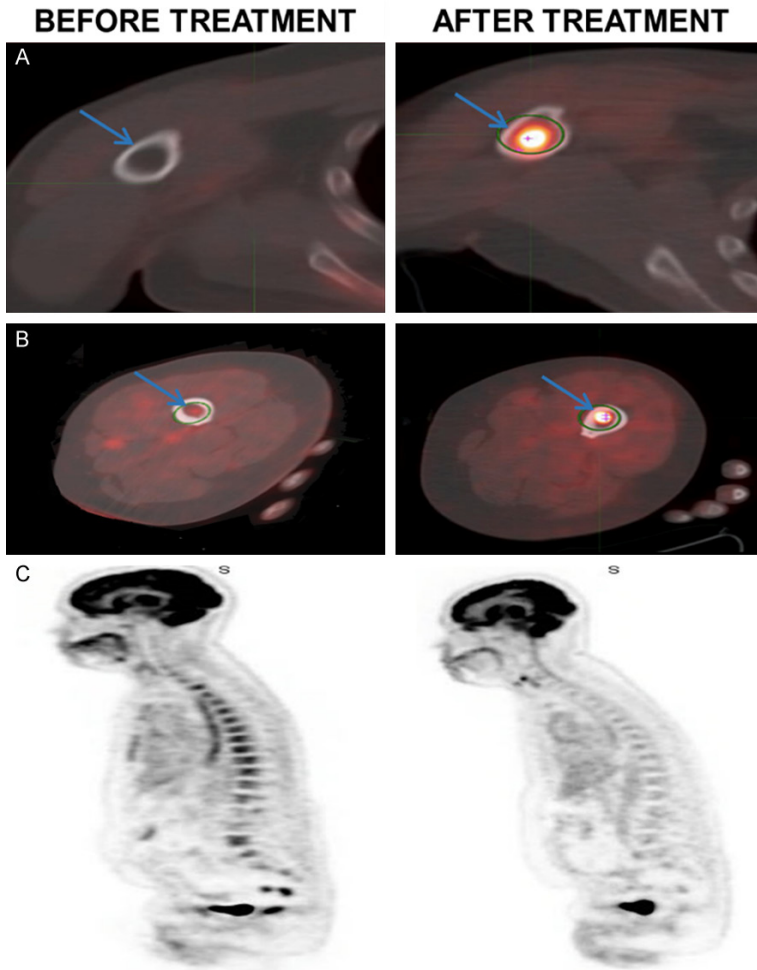


**Figure 1.** Case 1-PET imaging before and after therapy. A. Arrow points at a lesion in the right humerus femur with no  $^{18}\text{F}$ -FDG uptake before treatment and showing an  $\text{SUV}_{\text{max}}$  of 12 in the same area post treatment. B. Arrow shows an area in the left femur humerus with an  $\text{SUV}_{\text{max}}$  of 3 before treatment and  $\text{SUV}_{\text{max}}$  of 9.3 post treatment. C. Image depicts a pretreatment PET scan showing widespread axial skeletal disease and diffuse marrow  $^{18}\text{F}$ -FDG uptake. Post treatment PET scan shows response with therapy in axial skeleton and bone marrow.

apy followed by consolidation with tandem autologous stem cell transplants achieving a partial response. After 9 months, he had clinical and laboratory features consistent with disease relapse that was confirmed with increasing serum and urine monoclonal protein and free lambda light chains. PET/CT showed widespread BM hyper intensity along with multifocal increases throughout the axial skeleton and several new punctate lesions in the visualized extremities (**Figure 1**). BM analysis showed infiltration with over 90% malignant plasma cells. After multiple sequential lines of therapy, the patient had a 90% reduction in serum and

urine M protein and remarkable improvement in cytopenias. PET/CT post treatment showed minimal  $^{18}\text{F}$ -FDG uptake in BM with significant improvement in the innumerable previously noted axial lesions. However, there were two new lesions with high  $^{18}\text{F}$ -FDG uptake noted at the right humeral metaphysis and left femoral neck concerning for PD (**Figure 1**). The patient was deemed eligible for a relapsed MM Phase I clinical trial due to PD on last line of therapy based on development of a new  $^{18}\text{F}$ -FDG-avid lesion as listed in IMWG response criteria [8, 9]. However, a BM biopsy at this time in fact did not show any evidence of a plasma cell neoplasm by morphology or flow cytometry, confirming response to therapy. He was closely monitored off therapy and maintained this response for another 24 months.

Case 2

A 69-year-old male admitted to our hospital with anemia and worsening renal failure was found have IgG Kappa MM. He had a pre-treatment PET/CT imaging demonstrating diffuse, enhanced  $^{18}\text{F}$ -FDG BM uptake throughout the spine and pelvis and very low intracranial uptake. The  $\text{SUV}_{\text{max}}$  of the L4 vertebral body, right iliac crest and basal ganglia were measured as pre-treatment index lesions (**Figure 2**). With standard triplet induction therapy, he achieved a very good partial response (VGPR) based on clinical features, serum markers and results of BM biopsy as defined by the IMWG response criteria [8, 9] (**Table 1**). The patient experienced >98% reduction in serum and urine free light chains. Post-treatment PET/CT showed a significant reduction in  $^{18}\text{F}$ -FDG uptake throughout the BM and the reduction in plasma cell burden was confirmed on BM biopsy. However, there was a paradoxical increase

**BEFORE TREATMENT    AFTER TREATMENT**

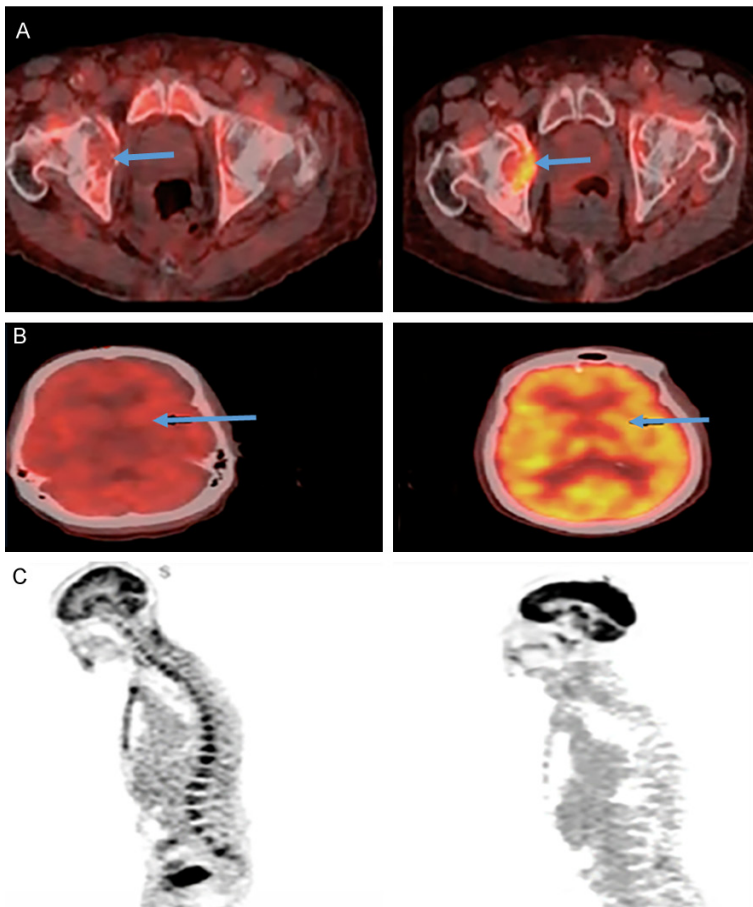


**Figure 2.** Case 2-PET imaging before and after therapy. A. Pelvic PET/CT showing diffuse increased bone marrow  $^{18}\text{F}$ -FDG uptake in the pelvis before therapy and interval development of a new focus of  $^{18}\text{F}$ -FDG uptake in right acetabulum on the post-therapy PET/CT. The bone marrow uptake returned to background  $^{18}\text{F}$ -FDG uptake after therapy. B. Brain PET/CT showing lower  $^{18}\text{F}$ -FDG uptake in the right basal ganglia (arrows) before therapy ( $\text{SUV}_{\text{max}} = 3.74$ ) and after therapy ( $\text{SUV}_{\text{max}} = 7.78$ ). C. Sagittal PET image of the upper body showing diffuse increased bone marrow  $^{18}\text{F}$ -FDG uptake through the entire spine. The correlative image after therapy illustrates the normal  $^{18}\text{F}$ -FDG in the spine with increased brain  $^{18}\text{F}$ -FDG uptake.

in  $^{18}\text{F}$ -FDG uptake in the right femoral head that was suspected to possibly represent PD and patient was considered eligible for a relapsed MM phase II clinical trial due PD on last line of therapy according to IMWG criteria [8, 9] (**Figure 2B**). Also noted was a relative increase in the intracranial uptake of  $^{18}\text{F}$ -FDG in comparison to pre-treatment PET/CT (**Figure 2C**). These findings were likely secondary to lack of  $^{18}\text{F}$ -FDG sequestration after successful anti-myeloma therapy and disappearance of myeloma-infiltrated marrow which leads to higher  $^{18}\text{F}$ -FDG availability for the brain and

right acetabulum lesion. On observation off treatment for a year after this, he was found to maintain the VGPR status with eventual resolution of the previously noted increased femoral  $^{18}\text{F}$ -FDG uptake, which was likely a non-tumor hyper metabolic bony lesion.

**Case 3**

A 65-year-old male with IgA lambda MM presented with multiple soft tissue plasmacytomas, a 4-cm hepatic lesion and extensive infiltration of BM with disease (**Figure 3A**). He achieved an initial partial response with standard induction therapy; however, just prior to stem cell collection, patient was noted to have PD with new plasmacytomas. He then underwent multiple sequential lines of salvage therapy (**Table 1**) and achieved over 98% reduction in myeloma markers and BM assessment showed significant reduction in plasma cell burden to 10-20% residual plasma cells from previous extensive marrow infiltration. PET/CT at this time showed resolution of the liver lesion and significant reduction in previously noted marrow activity; however, there was apparent worsening of disease in the appendicular skeleton and pelvic soft tissue masses that

previously showed minimal metabolism (**Figure 3B**). This would have been misinterpreted as PD by IMWG criteria while in actuality, he had achieved a significant reduction in myeloma disease burden.

**Discussion**

$^{18}\text{F}$ -FDG PET/CT plays an important role in MM where it combines functional imaging provided by PET with morphological evaluation assessed by CT. It enables the detection of metabolically active plasma cells both inside and outside the

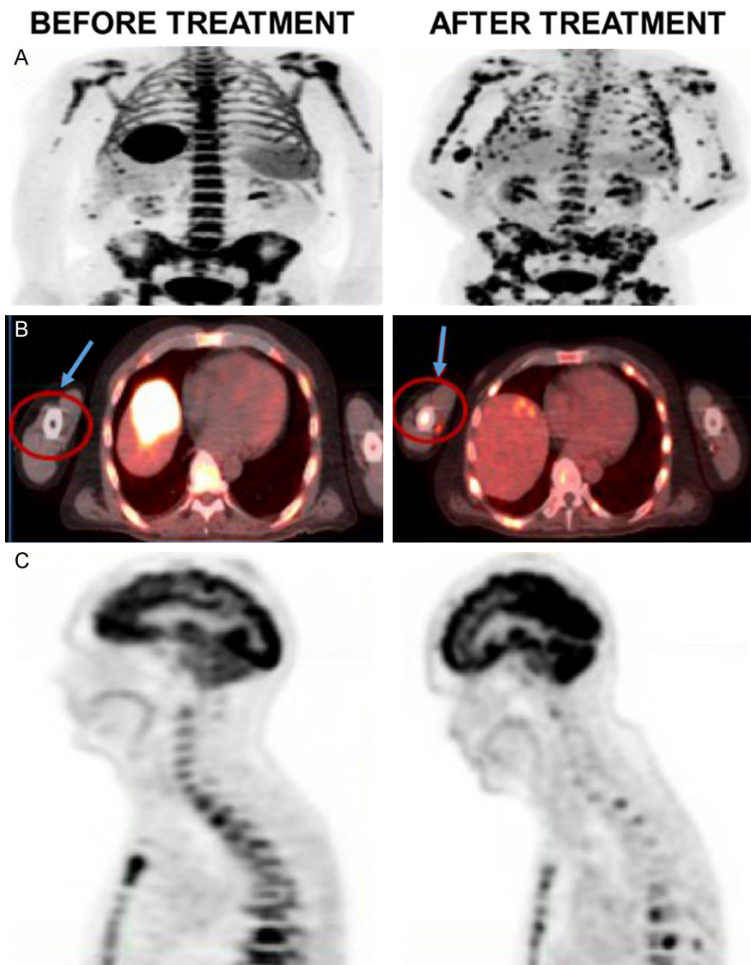


**Figure 3.** Case 3-PET imaging before and after therapy. A. PET/CT before treatment showing a hypermetabolic liver lesion and high  $^{18}\text{F}$ -FDG uptake in the bone marrow; Post treatment PET/CT shows interval development of hypermetabolic appendicular lesions with resolution of liver and bone marrow disease. B. An area in the right humerus with  $\text{SUV}_{\text{max}}$  of 2.5 pre-treatment and then an  $\text{SUV}_{\text{max}}$  of 8.5 post-treatment. C. Phenomenon of “cold-brain” noted in pre-treatment PET CT secondary to  $^{18}\text{F}$ -FDG tracer sequestration in the bone marrow heavily infiltrated with MM. PET/CT imaging post treatment shows an increase in brain  $^{18}\text{F}$ -FDG uptake after response to therapy in bone marrow.

BM, thus predicting patients’ clinical outcomes. The accuracy of  $^{18}\text{F}$ -FDG PET/CT imaging depends upon a number of factors that include optimal patient preparation, patient-specific metabolic features and adequate pharmacokinetics of  $^{18}\text{F}$ -FDG that together determine the tracer availability and uptake [2, 13, 14]. In highly metabolic bulky tumors or extensive tumor infiltrated marrow, there is radiographic tracer uptake and sequestration in the malignant areas. Consequently, there is less available tracer for uptake by physiologic or other pathologic sites. Diffuse increase in  $^{18}\text{F}$ -

FDG uptake in the marrow can significantly influence availability of  $^{18}\text{F}$ -FDG to other tissues including extra medullary tumor, given the large volume represented by the BM space. It has been shown that activation of the marrow by pegfilgrastim can reduce the available  $^{18}\text{F}$ -FDG to the tumor and lead to tumor SUV reduction, even with unchanged tumor metabolic rate [15]. Others defined a correction factor to calculate tumor SUV in the presence of high marrow  $^{18}\text{F}$ -FDG uptake [16]. A somewhat similar phenomenon can be seen with a high rate of false negative tumor detection by increased muscular uptake due to non-fasting state [17].

After therapy related eradication of myeloma infiltrated marrow, there is increased  $^{18}\text{F}$ -FDG tracer availability leading to an artefactual increase in  $^{18}\text{F}$ -FDG uptake at residual tumor sites. This may confound the interpretation of  $^{18}\text{F}$ -FDG PET/CT studies post-therapy.

Our cases illustrate the phenomenon of extensive BM infiltration by tumor leading to  $^{18}\text{F}$ -FDG tracer sequestration in the marrow, limiting its availability, not only to other pathologic sites, but also physiologic sites with healthy metabolically active tissues (i.e., brain). As described in Case 2, the absence of intracranial uptake (i.e. cold brain) in the pre-treatment PET scan was likely due to preferential distribution of tracer to the myeloma-infiltrated BM [18]. Subsequently, with treatment-based eradication of tumor, there is elimination of this aberrant tracer sequestration leading to normalization of  $^{18}\text{F}$ -FDG uptake in brain. Interestingly, the phenomenon of cold brain as a concomitant finding with bulky aggressive lymphoma has been described in some aggressive lymphomas and is associated with lower complete response

rate and shorter progression free survival [18-21].

MM therapy leads to elimination of tracer sequestration and causes an artefactual increase in metabolic activity at the sites of residual disease that could be misinterpreted as PD while in reality, there is significant treatment response by all other criteria. Such scenarios frequently prompt clinicians to reshape treatment strategies. Hence, it is important for oncologists to be cognizant of this potential situation, and to interpret  $^{18}\text{F}$ -FDG PET/CT studies in the context of other clinical and biomedical disease markers. The frequency of this sequestration phenomenon is unknown largely due to lack of frequent assessments of MM patients with PET/CT. Prospective trials that would study the extent of  $^{18}\text{F}$ -FDG sequestration at diagnosis, determine disease and host factors influencing this phenomenon (e.g. enhanced anaerobic glycolysis) as well as the influence of different anti-myeloma therapies on tumor metabolism of myeloma cells (reversal of 'Warburg effect') [22] and subsequent  $^{18}\text{F}$ -FDG uptake are warranted.

### Conclusion

Extensive BM infiltration by tumor leads to  $^{18}\text{F}$ -FDG tracer sequestration in the marrow, limiting its availability for uptake in other pathologic sites as well as physiologic sites with healthy metabolically active tissues.

Elimination of tracer sequestration with therapy and artefactual increase in metabolic activity at the sites of residual disease could be misinterpreted as PD based on IMWG criteria while in reality, the patient enjoys significant response to anti-myeloma therapy.

### Disclosure of conflict of interest

None.

**Address correspondence to:** Dr. Ehsan Malek, University Hospitals, Case Comprehensive Cancer Center, Case Western Reserve University, 11100, Euclid Avenue, Cleveland, OH 44106, USA. Tel: 216-844-8640; Fax: 216-201-5451; E-mail: exm301@case.edu

### References

[1] Durie BG, Waxman AD, D'Agnolo A and Williams CM. Whole-body  $^{18}\text{F}$ -FDG PET identifies high-

risk myeloma. *J Nucl Med* 2002; 43: 1457-1463.

- [2] Zamagni E, Patriarca F, Nanni C, Zannetti B, Englaro E, Pezzi A, Tacchetti P, Buttignol S, Perrone G, Brioli A, Pantani L, Terragna C, Carobolante F, Baccarani M, Fanin R, Fanti S and Cavo M. Prognostic relevance of  $^{18}\text{F}$  FDG PET/CT in newly diagnosed multiple myeloma patients treated with up-front autologous transplantation. *Blood* 2011; 118: 5989-5995.
- [3] Malek E, Sendilnathan A, Yellu M, Petersen A, Fernandez-Ulloa M and Driscoll JJ. Metabolic tumor volume on interim PET is a better predictor of outcome in diffuse large B-cell lymphoma than semiquantitative methods. *Blood Cancer J* 2015; 5: e326
- [4] Regelink JC, Minnema MC, Terpos E, Kamphuis MH, Raijmakers PG, Pieters-van den Bos IC, Heggelman BG, Nieveelstein RJ, Otten RH, van Lammeren-Venema D, Zijlstra JM, Arens AI, de Rooy JW, Hoekstra OS, Raymakers R, Sonneveld P, Ostelo RW and Zweegman S. Comparison of modern and conventional imaging techniques in establishing multiple myeloma-related bone disease: a systematic review. *Br J Haematol* 2013; 162: 50-61.
- [5] Bartel TB, Haessler J, Brown TL, Shaughnessy JD Jr, van Rhee F, Anaissie E, Alpe T, Angtuaco E, Walker R, Epstein J, Crowley J and Barlogie B. F18-fluorodeoxyglucose positron emission tomography in the context of other imaging techniques and prognostic factors in multiple myeloma. *Blood* 2009; 114: 2068-2076.
- [6] Susanibar S, Carlton V, Thanendrarajan S, Mohan M, Mathur P, Hoque S, Radhakrishnan M, van Rhee F, Zangari M, Davies FE, Kong KA, Morgan GJ, Alapat DV and Schinke C. Comparison of MRD detection by MFC, NGS and PET-CT in patients at different treatment stages for multiple myeloma. *Blood* 2016; 128: 377.
- [7] Kumar S, Paiva B, Anderson KC, Durie B, Landgren O, Moreau P, Munshi N, Lonial S, Bladé J and Mateos MV. International myeloma working group consensus criteria for response and minimal residual disease assessment in multiple myeloma. *Lancet Oncol* 2016; 17: e328-e346.
- [8] Cavo M, Terpos E, Nanni C, Moreau P, Lentzsch S, Zweegman S, Hillengass J, Engelhardt M, Usmani SZ and Vesole DH. Role of  $^{18}\text{F}$ -FDG PET/CT in the diagnosis and management of multiple myeloma and other plasma cell disorders: a consensus statement by the international myeloma working group. *Lancet Oncol* 2017; 18: e206-e217.
- [9] Rajkumar SV, Harousseau JL, Durie B, Anderson KC, Dimopoulos M, Kyle R, Blade J, Richardson P, Orlovski R, Siegel D, Jagannath S,

## PET imaging in multiple myeloma

- Facon T, Avet-Loiseau H, Lonial S, Palumbo A, Zonder J, Ludwig H, Vesole D, Sezer O, Munshi NC, San Miguel J; International Myeloma Workshop Consensus Panel 1. Consensus recommendations for the uniform reporting of clinical trials: report of the international myeloma workshop consensus panel 1. *Blood* 2011; 117: 4691-5.
- [10] Cook GJ, Maisey MN and Fogelman I. Normal variants, artefacts and interpretative pitfalls in PET imaging with 18-fluoro-2-deoxyglucose and carbon-11 methionine. *Eur J Nucl Med* 1999; 26: 1363-1378.
- [11] Dammacco F, Rubini G, Ferrari C, Vacca A and Racanelli V. <sup>18</sup>F-FDG PET/CT: a review of diagnostic and prognostic features in multiple myeloma and related disorders. *Clin Exp Med* 2015; 15: 1-18.
- [12] Palumbo A, Avet-Loiseau H, Oliva S, Lokhorst HM, Goldschmidt H, Rosinol L, Richardson P, Caltagirone S, Lahuerta JJ, Facon T, Bringhen S, Gay F, Attal M, Passera R, Spencer A, Offidani M, Kumar S, Musto P, Lonial S, Petrucci MT, Orłowski RZ, Zamagni E, Morgan G, Dimopoulos MA, Durie BG, Anderson KC, Sonneveld P, San Miguel J, Cavo M, Rajkumar SV and Moreau P. Revised international staging system for multiple myeloma: a report from international myeloma working group. *J Clin Oncol* 2015; 33: 2863-2869.
- [13] Delbeke D, Coleman RE, Guiberteau MJ, Brown ML, Royal HD, Siegel BA, Townsend DW, Berland LL, Parker JA, Hubner K, Stabin MG, Zubal G, Kachelriess M, Cronin V and Holbrook S. Procedure guideline for tumor imaging with <sup>18</sup>F-FDG PET/CT 1.0. *J Nucl Med* 2006; 47: 885-895.
- [14] Tomasi G, Turkheimer F and Aboagye E. Importance of quantification for the analysis of PET data in oncology: review of current methods and trends for the future. *Mol Imaging Biol* 2012; 14: 131-146.
- [15] Jacene HA, Ishimori T, Engles JM, Lebouilleux S, Stearns V and Wahl RL. Effects of pegfilgrastim on normal biodistribution of <sup>18</sup>F-FDG: preclinical and clinical studies. *J Nucl Med* 2006; 47: 950-956.
- [16] Teo BK, Badiee S, Hadi M, Lam T, Johnson L, Seo Y, Bacharach SL, Hasegawa BH and Franc BL. Correcting tumour SUV for enhanced bone marrow uptake: retrospective <sup>18</sup>F-FDG PET/CT studies. *Nucl Med Commun* 2008; 29: 359-366.
- [17] Lindholm H, Johansson O, Jonsson C and Jacobsson H. The distribution of FDG at PET examinations constitutes a relative mechanism: significant effects at activity quantification in patients with a high muscular uptake. *Eur J Nucl Med Mol Imaging* 2012; 39: 1685-1690.
- [18] Raghavendra M. Decreased brain FDG uptake in patients with diffuse large B cell lymphoma (cold brain) is associated with high risk disease and predicts poor response to R-CHOP chemotherapy. *Blood* 2012; 120: 1593-1593.
- [19] Hanaoka K, Hosono M, Shimono T, Usami K, Komeya Y, Tsuchiya N, Yamazoe Y, Ishii K, Tatsumi Y and Sumita M. Decreased brain FDG uptake in patients with extensive non-Hodgkin's lymphoma lesions. *Ann Nucl Med* 2010; 24: 707-711.
- [20] Nonokuma M, Kuwabara Y, Takano K, Tamura K, Ishitsuka K and Yoshimitsu K. Evaluation of regional cerebral glucose metabolism in patients with malignant lymphoma of the body using statistical image analysis. *Ann Nucl Med* 2014; 28: 950-960.
- [21] Shreve PD, Anzai Y and Wahl RL. Pitfalls in oncologic diagnosis with FDG PET imaging: physiologic and benign variants. *Radiographics* 1999; 19: 61-77.
- [22] El Arfani C, De Veirman K, Maes K, De Bruyne E and Menu E. Metabolic features of multiple myeloma. *Int J Mol Sci* 2018; 19.